Perception of UV-B by the *Arabidopsis* UVR8 Protein

Luca Rizzini *et al.*

Science **332**, 103 (2011);
DOI: 10.1126/science.1200660

Science (print ISSN 0036-8075; online ISSN 1095-9203) is published weekly, except the last week in December, by the American Association for the Advancement of Science, 1200 New York Avenue NW, Washington, DC 20005.

8. Single-letter abbreviations for the amino acid residues are as follows: A, Ala; C, Cys; D, Asp; E, Glu; F, Phe; G, Gly; H, His; I, Ile; K, Lys; L, Leu; M, Met; N, Asn; P, Pro; Q, Gln; R, Arg; S, Ser; T, Thr; V, Val; W, Trp; and Y, Tyr. In the mutants, other amino acids were substituted at certain locations; for example, H134R indicates that histidine at position 134 was replaced by arginine.
9. W. An, J. Kim, R. G. Roeder, *Cell* **117**, 735 (2004).
10. R. Métivier *et al.*, *Cell* **115**, 751 (2003).
11. M. Meininghaus, R. D. Chapman, M. Horndasch, D. Eick, *J. Biol. Chem.* **275**, 24375 (2000).
12. D. Baillat *et al.*, *Cell* **123**, 265 (2005).
13. S. Egloff *et al.*, *J. Biol. Chem.* **285**, 20564 (2010).
14. S. Egloff *et al.*, *Science* **318**, 1777 (2007).
15. N. Ohkura, M. Takahashi, H. Yaguchi, Y. Nagamura, T. Tsukada, *J. Biol. Chem.* **280**, 28927 (2005).
16. J. Côté, S. Richard, *J. Biol. Chem.* **280**, 28476 (2005).
17. N. Shaw *et al.*, *Nat. Struct. Mol. Biol.* **14**, 779 (2007).
18. R. Sprangers, M. R. Groves, I. Sinning, M. Sattler, *J. Mol. Biol.* **327**, 507 (2003).
19. Y. Z. Yang *et al.*, *Mol. Cell* **40**, 1016 (2010).
20. These studies were supported by the HHMI (to D.R.) and grants from NIH (GM-37120 to D.R. and GM-71166 to R.J.S.). R.B. is a fellow of the Helen Hay Whitney foundation. D.E. was supported by Deutsche Forschungsgemeinschaft (SFB/Transregio-5, SFB684) and José Carreras Leukämie-Stiftung eV. We thank L. Vales, E. Lecona, and P. Voigt for careful reading of the manuscript; R. D. Chapman and K. Burger for technical support; and members of the Reinberg lab for critical commentaries during the development of this project. RNA-seq data have been deposited in the National Center for Biotechnology Information's Gene Expression Omnibus as GEO series GSE27315.

Supporting Online Material

www.sciencemag.org/cgi/content/full/332/6025/99/DC1
Materials and Methods
Figs. S1 to S5
References

10 January 2011; accepted 22 February 2011
10.1126/science.1202663

Perception of UV-B by the *Arabidopsis* UVR8 Protein

Luca Rizzini,[1]* Jean-Jacques Favory,[1]* Catherine Cloix,[2] Davide Faggionato,[3] Andrew O'Hara,[2] Eirini Kaiserli,[2]† Ralf Baumeister,[3,4] Eberhard Schäfer,[1,4] Ferenc Nagy,[5,6] Gareth I. Jenkins,[2] Roman Ulm[1,4,7]‡

To optimize their growth and survival, plants perceive and respond to ultraviolet-B (UV-B) radiation. However, neither the molecular identity of the UV-B photoreceptor nor the photoperception mechanism is known. Here we show that dimers of the UVR8 protein perceive UV-B, probably by a tryptophan-based mechanism. Absorption of UV-B induces instant monomerization of the photoreceptor and interaction with COP1, the central regulator of light signaling. Thereby this signaling cascade controlled by UVR8 mediates UV-B photomorphogenic responses securing plant acclimation and thus promotes survival in sunlight.

Sunlight is of primary importance to sessile plants, both as an energy source to fuel photosynthesis and as an informational signal influencing their entire life cycle. Several families of plant photoreceptors have evolved that monitor light ranging from ultraviolet-B (UV-B) to the near infrared and allow optimal adaptation to light (*1*–*3*). Plant perception of UV-B radiation as an environmental stimulus is known to affect growth and development (*1*, *2*, *4*–*8*); however, no photoreceptor protein specifically sensing UV-B radiation has yet been molecularly identified.

We previously provided evidence for a specific pathway mediating molecular and physiological responses of *Arabidopsis* to low-level UV-B, involving the bZIP transcription factor ELONGATED HYPOCOTYL 5 (HY5), the E3 ubiquitin ligase CONSTITUTIVELY PHOTOMORPHOGENIC 1 (COP1), and the β-propeller protein UV RESISTANCE LOCUS 8 (UVR8) (*4*, *9*–*11*). UVR8 contains sequence similarity to the human guanine nucleotide exchange factor Regulator of Chromatin Condensation 1 (RCC1) (*12*); however, available evidence suggests that RCC1 and UVR8 differ in activity and function (*1*).

cop1 and *uvr8* mutants show no UV-B photomorphogenic responses, and COP1 and UVR8 proteins interact within minutes in planta in a strictly UV-B–dependent manner (*4*). Moreover, both proteins were found to accumulate in the nucleus under supplementary UV-B radiation (*11*, *13*). These properties are reminiscent of known photoreceptors (*3*, *4*). In agreement with such a function, we found that the UVR8-COP1 interaction also takes place in protein extracts in a very rapid, UV-B–dependent manner (Fig. 1A), mimicking the in planta situation described before (*4*). This feature allowed us to further investigate the requirements for this early response to UV-B. We UV-B–irradiated separately protein extracts containing either yellow

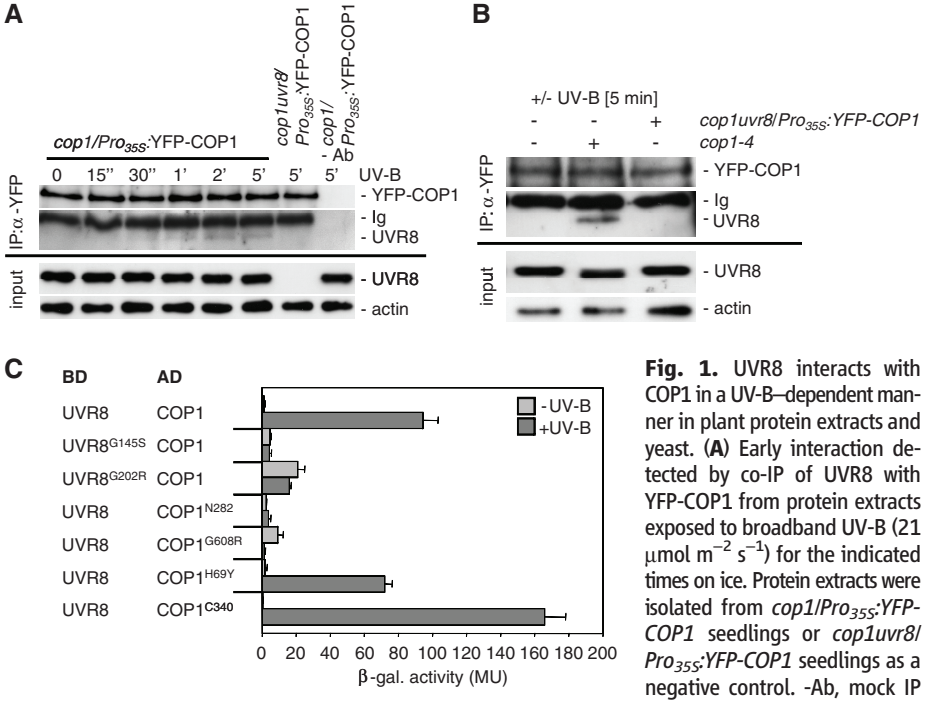

Fig. 1. UVR8 interacts with COP1 in a UV-B–dependent manner in plant protein extracts and yeast. (**A**) Early interaction detected by co-IP of UVR8 with YFP-COP1 from protein extracts exposed to broadband UV-B (21 μmol m^{-2} s^{-1}) for the indicated times on ice. Protein extracts were isolated from *cop1/Pro35S:YFP-COP1* seedlings or *cop1uvr8/Pro35S:YFP-COP1* seedlings as a negative control. -Ab, mock IP without antibodies to YFP; Ig, immunoglobulins. (**B**) Protein extracts were isolated from *cop1-4* and *cop1uvr8/Pro35S:YFP-COP1* seedlings and treated separately with UV-B (+, 21 μmol m^{-2} s^{-1}) or not (-) on ice. In combinations of the extracts, co-IP of UVR8 with YFP-COP1 was detected only when extracts containing UVR8 (*cop1-4*) were UV-B–treated and not when only YFP-COP1 was treated (*cop1uvr8/Pro35S:YFP-COP1*). (**C**) Yeast two-hybrid interaction of UVR8 and COP1 is UV-B–dependent (16 hours, 1.5 μmol m^{-2} s^{-1}) and is impaired in nonfunctional UVR8 and COP1 mutant proteins. β-gal., β-galactosidase; MU, Miller units.

[1]Faculty of Biology, Institute of Biology II, University of Freiburg, D-79104 Freiburg, Germany. [2]Institute of Molecular Cell and Systems Biology, University of Glasgow, Glasgow G12 8QQ, UK. [3]Faculty of Biology, Institute of Biology III, and Faculty of Medicine, ZBMZ, University of Freiburg, D-79104 Freiburg, Germany. [4]BIOSS Centre for Biological Signalling Studies, University of Freiburg, D-79104 Freiburg, Germany. [5]Institute of Plant Biology, Biological Research Centre, H-6726 Szeged, Hungary. [6]School of Biological Sciences, University of Edinburgh, Edinburgh EH9 3JR, UK. [7]Department of Botany and Plant Biology, University of Geneva, Sciences III, CH-1211 Geneva 4, Switzerland.

*These authors contributed equally to this work.
†Present address: The Salk Institute for Biological Studies, La Jolla, CA 92037, USA.
‡To whom correspondence should be addressed. E-mail: roman.ulm@unige.ch

fluorescent protein (YFP)–COP1 but not UVR8 (*cop1 uvr8*/*Pro*$_{35S}$*:YFP-COP1* line), or UVR8 but not YFP-COP1/COP1 (*cop1* mutant), and then mixed them with non-irradiated extracts containing the respective partner protein, followed by coimmunoprecipitation (co-IP) assays of UVR8 using antibodies to YFP (Fig. 1B). The results showed that UV-B irradiation of extracts containing UVR8 was both required and sufficient for the interaction with YFP-COP1 (Fig. 1B), indicating a primary function of UVR8 in UV-B signal perception.

The UVR8-COP1 interaction thus provided a robust readout to test whether an initial UV-B response could be synthetically generated in an heterologous system. We used the yeast two-hybrid test system in *Saccharomyces cerevisiae* to further examine the UVR8-COP1 interaction. It is necessary to note that yeast does not contain a COP1 homolog (*14*) nor a UVR8 protein [a structurally related protein is a bona fide RCC1 homolog (*12*, *15*)]. In yeast, UVR8 also interacted with COP1 in the presence of UV-B but not in its absence (Fig. 1C and fig. S1). This resembles the red- and blue light–specific interactions of phytochrome and cryptochrome photoreceptors with their early targets in yeast (*16*–*18*) and strongly indicates that UVR8 and COP1 are sufficient to constitute an early UV-B–specific response in a nonplant heterologous system.

Consistent with the evidence in planta (*4*, *10*), UVR8 proteins containing mutations that impair UV-B–induced photomorphogenesis in vivo, namely *uvr8-2* (UVR8^{N400}), *uvr8-9* (UVR8^{G202R}) and *uvr8-15* (UVR8^{G145S}), did not interact with wild-type COP1 (Fig. 1C and fig. S1). Similarly, nonfunctional mutant COP1 proteins representing *cop1-4* (COP1^{N282}) and *cop1-19* (COP1^{G608R}) did not interact with wild-type UVR8 (Fig. 1C and fig. S1). The failure of UVR8 interaction with the N-terminal 282 amino acids (COP1^{N282}) in the absence of C-terminal WD40 repeats indicated a requirement for this domain for the interaction. Consistent with this notion, expression of the C-terminal 340 amino acids (COP1^{C340}) comprising only WD40 repeats demonstrated that the WD40 domain of COP1 is sufficient for its interaction with UVR8 under UV-B (Fig. 1C and fig. S1). Moreover, COP1^{H69Y} still interacted with UVR8 in a UV-B–specific manner (Fig. 1C), in agreement with the ability of the corresponding *cop1*^{eid6} mutant to respond to UV-B (*11*). Together with the results from cell-free protein extracts, UV-B–specific interaction of UVR8 with COP1 in yeast further supports the conclusion that UVR8 constitutes a plant UV-B receptor.

Previously, we described constitutive UVR8 dimers in mustard by bimolecular fluorescence complementation (BiFC) in transient assays (*4*). However, reconstitution of a functional YFP in the BiFC assay is practicably irreversible, and thus dynamics cannot be captured (*19*). We therefore turned to more appropriate experimental systems to investigate UVR8 dimer dynamics. First, endogenous UVR8 protein was coimmunoprecipitated with CFP-UVR8 from *Pro*$_{35S}$*:CFP-UVR8* transgenic lines in a wild-type background (Fig. 2A). Negligible endogenous UVR8 was detected in the coimmunoprecipitates under supplemental UV-B, indicating a marked reduction in CFP-UVR8–UVR8 interaction that represents dimer formation (Fig. 2A). This strongly indicated the presence of UVR8 as a dimer in white light without UV-B and its monomerization under supplemental UV-B. In agreement with this indication, analysis of non–heat-denatured protein extracts revealed a marked accumulation of UVR8 monomers under supplemental UV-B as compared with minus–UV-B controls (Fig. 2B, upper panel). In these experiments, however, UVR8 was almost undetectable in the minus–UV-B control (note the weak cross-reacting band that is also detectable in the *uvr8-6* null mutant). In contrast to this observation, but in agreement with previously published data (*4*, *13*), UVR8 protein levels were similar when parallel samples were denatured by boiling (Fig. 2B, upper panel). Thus, our antibodies to UVR8 clearly failed to detect the epitope on non–UV-B-irradiated UVR8. When the gel was irradiated with UV-B before protein transfer to the membrane, a prominent band of higher molecular weight was detected in the same extracts under these conditions. This suggested that UV-B irradiation of UVR8 increased accessibility of the epitope on endogenous UVR8 (Fig. 2B, lower panel) and thus indicated an in-gel conformational change in UVR8 upon UV-B perception linked to the in vivo monomerization of the UVR8 dimers. UVR8 monomerization was found to be a very rapid process detectable after 5 s of UV-B treatment of

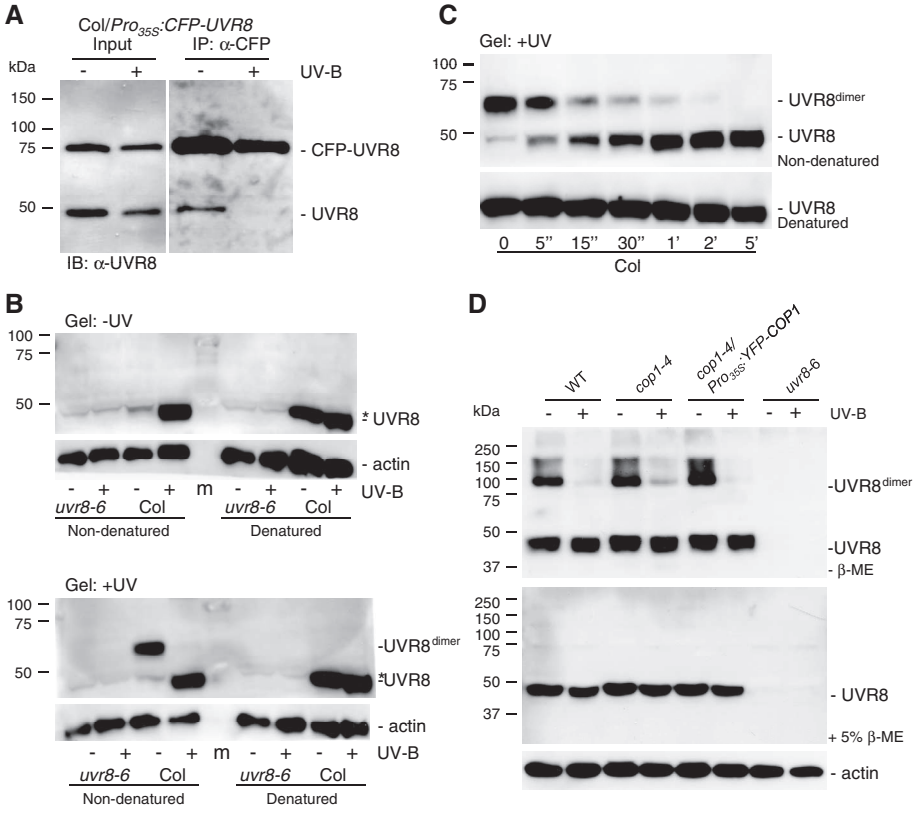

Fig. 2. UVR8 forms dimers in the absence of UV-B and monomerizes in a UV-B–dependent manner. (**A**) Co-IP of endogenous UVR8 with CFP-UVR8 from Col/*Pro*$_{35S}$*:CFP-UVR8* was reduced when seedlings were treated with UV-B (1 hour, 21 μmol m^{-2} s^{-1}). (**B**) UVR8 dimers were detectable in non–heat-denatured samples of *Arabidopsis* protein extracts not treated with UV-B (-), but only if the protein gel was irradiated by UV-B after the gel run (15 min, 21 μmol m^{-2} s^{-1}) and before transfer to a membrane (lower panel). Under non–heat-denatured conditions, the apparent UVR8 dimer size is smaller than the expected 94 kD, indicating that the electrophoretic behavior of the not-fully-denatured UVR8 dimer is anomalous. Treatment of protein extracts by UV-B (5 min, 21 μmol m^{-2} s^{-1}) resulted in UVR8 monomerization. Parallel denatured samples demonstrated equal amounts of UVR8 protein. Actin levels are shown as loading controls. (**C**) Time course analysis of UVR8 monomerization in cell-free plant extracts after exposure to UV-B (21 μmol m^{-2} s^{-1}) on ice for the indicated times. The gel blot of heat-denatured proteins shows equal UVR8 protein amounts. (**D**) UVR8 dimers are cross-linked by DSP, which is reversible by reducing agents (β-ME), showing equal protein amounts. UV-B (5 min, 21 μmol m^{-2} s^{-1}) resulted in a decrease of UVR8 dimers, which was independent of COP1. The UV-B irradiation conditions that result in UVR8 monomerization correspond to the ones causing UVR8-dependent gene expression changes in vivo [SOM and (*4*, *9*, *11*)].

protein extracts on ice (Fig. 2C). Moreover, UVR8 monomerization was fluence rate–dependent and displayed a reciprocal relationship between treatment duration and fluence rate under the tested conditions (fig. S2). Finally, the decrease of UVR8 dimers upon UV-B irradiation was also apparent when proteins were cross-linked using dithiobis(succinimidyl propionate) (DSP) (Fig. 2D, upper panel), which generates reversible protein-protein cross-links that can be cleaved by β-mercaptoethanol (β-ME) (Fig. 2D, lower panel).

To investigate whether COP1 affects UVR8 monomerization, we used DSP cross-linking on protein extracts from *cop1-4* seedlings treated or not treated with UV-B. UVR8 monomerization was similar in *cop1-4* and the wild type, demonstrating that UVR8 monomerization does not require functional COP1 protein (Fig. 2D). Together, these results demonstrate rapid monomerization of UVR8 dimers, probably as the result of the direct perception of UV-B by UVR8 and an associated conformational change (as suggested by epitope detection only after UV-B irradiation of UVR8 before or after electrophoresis, or after heat denaturation).

To further challenge the conclusion that the UVR8 protein has UV-B photoreceptor properties, we examined whether UVR8 monomerization also happens in heterologous systems. Indeed, dimers were detected when UVR8 was expressed in yeast cells grown under conditions devoid of UV-B radiation. In contrast, only UVR8 monomers were found after yeast was irradiated with supplemental UV-B (Fig. 3A). UVR8 mutants that are nonfunctional and incapable of interacting with COP1 were also unable to form dimers (Fig. 3A). Similar to yeast, UVR8 dimers from transfected human embryonic kidney (HEK) 293T cells monomerized in response to UV-B (Fig. 3B).

Aromatic amino acids absorb UV-B radiation. Tryptophan, with an absorption maximum in solution at around 280 nm (which extends to 300 nm and is likely to be further shifted in a protein environment), is particularly suited as a potential UV-B chromophore (*20*, *21*) (UV-B: 280 to 315 nm). This is in agreement with a recent action spectrum for *HY5* gene activation by UVR8 that identified peaks at 280 and 300 nm (*22*). Structure modeling according to the structurally related human RCC1 protein (*12*, *23*) identified 14 tryptophans of UVR8 (the similarly sized human RCC1 contains only four), all located at the top of the predicted UVR8 β-propeller structure (fig. S3), with a particularly intriguing cluster at positions 233, 285, and 337 in the center of the protein structure (Fig. 3C and fig. S3). To examine the potential involvement of these tryptophans in UV-B sensing, they were targeted by mutagenesis, changing them to alanine (UVR8^{W285A} and UVR8^{W337A}) or phenylalanine (UVR8^{W233F}, UVR8^{W285F}, and UVR8^{W337F}). Whereas the W285A, W337A, and W233F mutations abrogated dimerization and W337F still showed UV-B–induced monomerization, mutation of tryptophan-285 to phenylalanine resulted in a constitutive UVR8 dimer with no response to UV-B (Fig. 3D and fig. S4). Yeast two-hybrid analysis revealed a constitutive interaction of UVR8^{W285A} with COP1, although not as strong as the UV-B–induced interaction of the wild-type proteins, and absolutely no interaction of UVR8^{W285F} with COP1 (Fig. 3E). The latter was of particular interest, because dimer formation indicated that the overall structure was largely unaffected by the moderate single tryptophan-to-phenylalanine exchange, whereas UV-B perception was abrogated (absorption maximum of phenylalanine at 257 nm).

Taken together, the results presented here provide strong evidence that plant perception of UV-B is mediated by UVR8 as a UV-B–specific photoreceptor, and they support a tryptophan-based perception mechanism, with tryptophan-285 as a key residue. The UV-B–driven monomerization of the UVR8 dimers signals the receptor activation, which then is followed by interaction with COP1 to relay the signal. The constitutive expression of UVR8 throughout the plant (fig. S5) (*4*, *13*) allows any plant organ to immediately respond to UV-B exposure and to mount protective measures. UVR8 proteins are broadly present and well conserved among plants (fig. S6). This raises the intriguing possibility that, together with the development of an ozone layer in the stratosphere of Earth (*24*), the evolution of terrestrial plants may be coincident with the acquisition of the UV-induced responses mediated by the UVR8 UV-B photoreceptor.

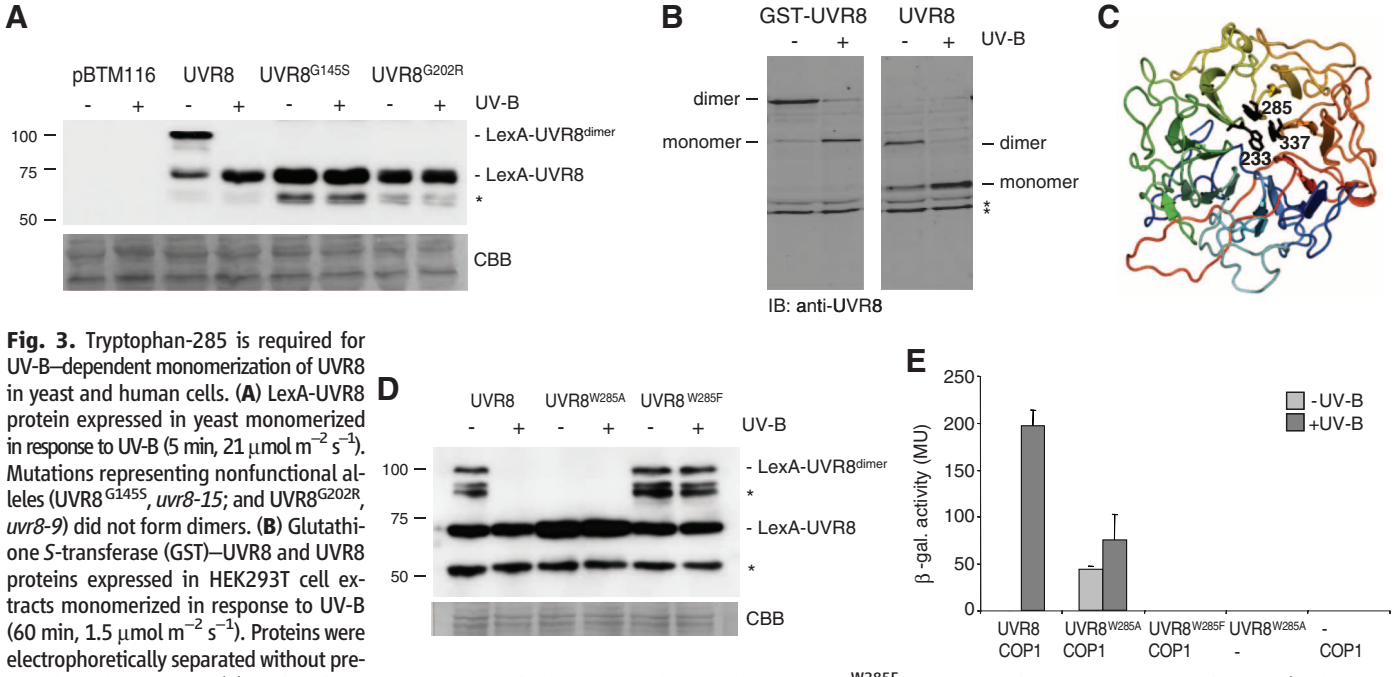

Fig. 3. Tryptophan-285 is required for UV-B–dependent monomerization of UVR8 in yeast and human cells. (**A**) LexA-UVR8 protein expressed in yeast monomerized in response to UV-B (5 min, 21 μmol m^{-2} s^{-1}). Mutations representing nonfunctional alleles (UVR8^{G145S}, *uvr8-15*; and UVR8^{G202R}, *uvr8-9*) did not form dimers. (**B**) Glutathione *S*-transferase (GST)–UVR8 and UVR8 proteins expressed in HEK293T cell extracts monomerized in response to UV-B (60 min, 1.5 μmol m^{-2} s^{-1}). Proteins were electrophoretically separated without previous heat denaturation. (**C**) Predicted structure of UVR8, including in particular the tryptophan cluster with the tryptophan-233, -285, and -337 residues. (**D**) Dependence on tryptophan-285 for UV-B–mediated UVR8 monomerization in yeast. UVR8^{W285A} did not form dimers, whereas UVR8^{W285F} formed dimers but did not monomerize in response to UV-B (5 min, 21 μmol m^{-2} s^{-1}). (**E**) UVR8^{W285A} interacted constitutively with COP1 in a yeast two-hybrid assay, whereas UVR8^{W285F} was impaired in its interaction with COP1 (16 hours of UV-B, 1.5 μmol m^{-2} s^{-1}). (A) and (D) Proteins were electrophoretically separated without previous heat denaturation. The protein gel blot was probed with an antibody to LexA, and the Coomassie brilliant blue (CBB)–stained membrane is shown as a loading control. In (A), (B), and (D), the asterisks indicate degradation products.

References and Notes

1. G. I. Jenkins, *Annu. Rev. Plant Biol.* **60**, 407 (2009).
2. R. Ulm, F. Nagy, *Curr. Opin. Plant Biol.* **8**, 477 (2005).
3. C. Kami, S. Lorrain, P. Hornitschek, C. Fankhauser, *Curr. Top. Dev. Biol.* **91**, 29 (2010).
4. J. J. Favory *et al.*, *EMBO J.* **28**, 591 (2009).
5. J. J. Wargent, V. C. Gegas, G. I. Jenkins, J. H. Doonan, N. D. Paul, *New Phytol.* **183**, 315 (2009).
6. H. Frohnmeyer, D. Staiger, *Plant Physiol.* **133**, 1420 (2003).
7. N. D. Paul, D. Gwynn-Jones, *Trends Ecol. Evol.* **18**, 48 (2003).
8. H. Tong *et al.*, *Proc. Natl. Acad. Sci. U.S.A.* **105**, 21039 (2008).
9. R. Ulm *et al.*, *Proc. Natl. Acad. Sci. U.S.A.* **101**, 1397 (2004).
10. B. A. Brown *et al.*, *Proc. Natl. Acad. Sci. U.S.A.* **102**, 18225 (2005).
11. A. Oravecz *et al.*, *Plant Cell* **18**, 1975 (2006).
12. D. J. Kliebenstein, J. E. Lim, L. G. Landry, R. L. Last, *Plant Physiol.* **130**, 234 (2002).
13. E. Kaiserli, G. I. Jenkins, *Plant Cell* **19**, 2662 (2007).
14. C. Yi, X. W. Deng, *Trends Cell Biol.* **15**, 618 (2005).
15. M. Fleischmann *et al.*, *Mol. Gen. Genet.* **227**, 417 (1991).
16. S. Shimizu-Sato, E. Huq, J. M. Tepperman, P. H. Quail, *Nat. Biotechnol.* **20**, 1041 (2002).
17. A. Hiltbrunner *et al.*, *Curr. Biol.* **15**, 2125 (2005).
18. H. Liu *et al.*, *Science* **322**, 1535 (2008).
19. T. K. Kerppola, *Nat. Rev. Mol. Cell Biol.* **7**, 449 (2006).
20. D. Creed, *Photochem. Photobiol.* **39**, 537 (1984).
21. E. Fritsche *et al.*, *Proc. Natl. Acad. Sci. U.S.A.* **104**, 8851 (2007).
22. B. A. Brown, L. R. Headland, G. I. Jenkins, *Photochem. Photobiol.* **85**, 1147 (2009).
23. L. Renault *et al.*, *Nature* **392**, 97 (1998).
24. J. Rozema, J. van de Staaij, L. O. Björn, M. Caldwell, *Trends Ecol. Evol.* **12**, 22 (1997).

25. We thank L.-O. Essen, J. Paszkowski, and T. Kunkel for helpful comments and advice, and P. King for editing the manuscript. This research was supported by grants from the UK Biotechnology and Biological Sciences Research Council and the Leverhulme Trust to G.I.J.; the Scottish Universities Life Science Alliance and the Hungarian Scientific Research Fund (OTKA-81399) to F.N.; the Sonderforschungsbereich (SFB) 592 to R.B.; the Excellence Initiative of the German Federal and State Governments (EXC 294) and the SFB 746 to R.B., E.S., and R.U.; and the Emmy Noether Programme of the Deutsche Forschungsgemeinschaft (grant UL341/1-1) to R.U.

Supporting Online Material

www.sciencemag.org/cgi/content/full/332/6025/103/DC1
Materials and Methods
Figs. S1 to S7
References

19 November 2010; accepted 18 February 2011
10.1126/science.1200660

Bacteria-Phage Antagonistic Coevolution in Soil

Pedro Gómez[1,2]* and Angus Buckling[1,3]

Bacteria and their viruses (phages) undergo rapid coevolution in test tubes, but the relevance to natural environments is unclear. By using a "mark-recapture" approach, we showed rapid coevolution of bacteria and phages in a soil community. Unlike coevolution in vitro, which is characterized by increases in infectivity and resistance through time (arms race dynamics), coevolution in soil resulted in hosts more resistant to their contemporary than past and future parasites (fluctuating selection dynamics). Fluctuating selection dynamics, which can potentially continue indefinitely, can be explained by fitness costs constraining the evolution of high levels of resistance in soil. These results suggest that rapid coevolution between bacteria and phage is likely to play a key role in structuring natural microbial communities.

Host-parasite antagonistic coevolution—the reciprocal evolution of host defense and parasite counter-defense—is theoretically crucial to a range of ecological and evolutionary processes, including population dynamics and extinction risk, the evolution of diversity and speciation, the evolution of sex and mutation rates, and the evolutionary ecology of pathogen virulence (*1*–*4*). A number of excellent studies have inferred the operation of host-parasite coevolution in natural populations from patterns of local adaptation of parasites to their hosts in space and time (*5*–*10*). However, genetic variation between the host populations in space and time may be driven by parasite-imposed selection but could equally be driven by neutral process or additional selection pressures. A direct demonstration of coevolution requires evidence of host adaptation to parasites as well as parasite adaptation to hosts.

Antagonistic coevolution between bacteria and their ubiquitous parasites, bacteriophage (phage), is likely to be of particularly broad importance because of their extremely rapid rates of evolution (*3*, *11*)—the key role played by bacteria in ecosystem functioning—and the therapeutic use of phages as "evolving" antibiotics in agricultural and clinical contexts (*11*). Both the dynamics and consequences of coevolution between bacteria and viruses have been extensively studied in the laboratory (*12*, *13*), but little is known about the extent or role of rapid bacteria-phage coevolution in natural populations (*14*, *15*). Given that phages are typically highly specific to bacteria species and even genotypes (*11*) and the massive amount of diversity present in microbial communities (*16*), a given interacting bacteria and phage population is likely to make up a tiny fraction of the microbial community. It is therefore unclear whether phages, which only encounter hosts passively, impose sufficient selection on bacteria for rapid coevolution to occur.

We used a "mark-recapture" approach (*17*) to follow the ecological and evolutionary dynamics of a soil bacteria clone, *Pseudomonas fluorescens* SBW25, and a naturally associated lytic bacteriophage clone SBW25ϕ2 (*18*) in soil microcosms. Despite these organisms having been used extensively for in vitro evolution studies (*13*), they were frozen shortly after their original isolation and hence would have undergone little laboratory adaptation before our experiment. The

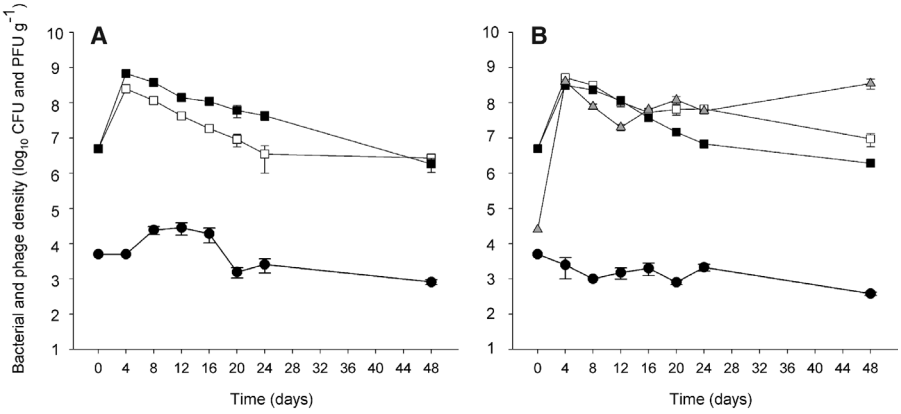

Fig. 1. Population dynamics of the bacterial and phage populations. Connected symbols show densities through time [mean $\log_{10}$(colony forming units/g soil) for bacteria or $\log_{10}$(plaque forming units/g soil) for phage, ± SEM] of phage SBW25ϕ2 (●); *P. fluorescens* SBW25 evolved in the presence (■) or absence (□) of phage; and the culturable fraction of the natural community (▲). Populations were evolved in the (**A**) absence and (**B**) presence of the natural community.

[1]Department of Zoology, University of Oxford, Oxford OX1 3PS, UK. [2]Centro de Edafología y Biología Aplicada del Segura, Consejo Superior de Investigaciones Científicas (CEBAS-CSIC), Murcia (Espinardo) 30100, Spain. [3]Biosciences, University of Exeter, Penryn TR10 9EZ, UK.

*To whom correspondence should be addressed. E-mail: pedro.gomezlopez@zoo.ox.ac.uk